PETTER JOHANSSON

PAIR ANNIHILATION IN A LASER PULSE

PAIR ANNIHILATION IN A LASER PULSE

PETTER JOHANSSON

Master's thesis in Physics

Department of Physics
Umeå University

Spring 2011

Petter Johansson: *Pair annihilation in a laser pulse,* Master's thesis in Physics, © Spring 2011

SUPERVISORS:
Anton Ilderton
Mattias Marklund

EXAMINATOR:
Michael Bradley

LOCATION:
Umeå University

TIME FRAME:
Spring 2011

ABSTRACT

The thesis analyses the process of pair annihilation into one photon in a laser pulse. The theory of how to include pulse shapes in Strong Field QED and the resulting cross section is presented. The cross section is calculated and estimated for lasers of ELI and XFEL facilites.

It is found that the effect may be experimentally verifiable at high frequency XFEL facilities for very finely tuned particle kinematics, but negligible at high intensity optical laser facilities such as ELI.

CONTENTS

1 OVERVIEW

The advent of Quantum Electrodynamics (QED) in the 1930's has redefined the way we understand nature, describing the way in which light and matter interact with each other. It has managed to unite Quantum Mechanics with Special Relativity and described many effects such as Lamb shift, the Casimir effect, virtual photons and Compton scattering to incredible precision compared with experiments.

A subject which QED is adept at describing is that of intense electromagnetic fields, so called *strong field QED*. The influence of external fields give rise to two types of effects: Modifications to effects present without fields, and completely new effects never seen in vacuum. An interesting example of the latter kind is Schwinger pair production, which describes how in an electric background field of strength E there is a probability for a virtual particle pair becoming real through absorbing energy and momenta from the field (see Figure 1 and [1, 2]). The probability for this to occur is proportional to $\exp\left(-\pi E_c/E\right)$ where $E_c = 1.3 \times 10^{16}\,\mathrm{V/cm}$ is a critical field strength above which pair production becomes abundant [3] and one example of a scale for when Strong Field QED models are relevant.

A lot of other effects from these models have also been theorised, a few of which along with relevant references are *a*) Stimulated pair production, modeling an external photon producing a particle-antiparticle pair within a background field [4]. This effect was first spotted at the Stanford Linear Accelerator Center (SLAC) in 1999 [5]. *b*) Trident pair production, wherein a par-

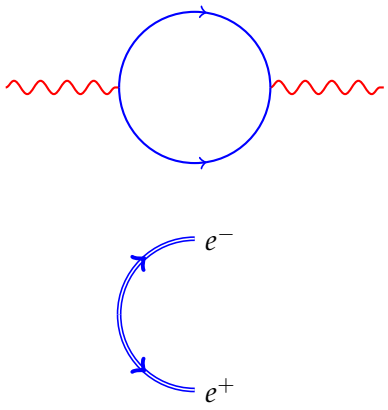

Figure 1: Top: A photon fluctuating into an electron-positron pair. Bottom: Two real particles are created in a background field. Particles in background fields are represented by double lines.

ticle in a field emits a photon which splits into a new particle-antiparticle pair [6]. *c*) Nonlinear Compton scattering, or particles scattering against photons in a field [7]. Like stimulated pair production this effect has been experimentally verified, in 1998 [8], though plans to repeat these experiments exist.

Modern laser facilities are now beginning to reach required laser powers and intensities for strong field effects such as these to be of importance. For instance there is the Extreme Light Infrastructure (ELI) project[1], which consists of a number of planned facilities around Europe meant to further research in radiography, hadron therapy and more as well as test predictions of high field physics. Lasers in ELI are planned to approach fields E of $E \lesssim 10^{-2}E_c$ which will be combined with a high-energy linear accelerator. Another upcoming facility is the European X-ray Free Electron Laser (XFEL) in Germany[2], using flashes of high-energy photons to study formation of molecules, complex biomodules and extreme states of matter and also will be able to collide beams with high-energy particles from a linear accelerator. These lasers, while still of strengths a few orders of magnitude below E_c, or the Schwinger limit, present good opportunities to verify Strong Field QED effects.

In this thesis the cross section for pair annihilation into a single photon in shaped laser pulses is studied for lasers that these two facilities will use. The underlying theory is covered in Chapter 2 and then the results for the XFEL and ELI lasers are calculated in Chapters 3 and 4 respectively. Conclusions are presented in Chapter 5.

We begin by introducing the process in the absence of fields.

1.1 PAIR ANNIHILATION IN VACUUM

Pair annihilation is one of the simplest predictions of QED and as such has been extensively studied and experimentally verified many times over [9]. In the process, a particle-antiparticle pair interact with each other by annihilating and producing new particles of other types, as allowed by conservation of total spin, charge, momentum and energy. Consider annihilation into photons, in vacuum at least two photons must be emitted in the process, since momentum conservation $p_\mu + p'_\mu = k'_\mu$ for an incoming particle pair p_μ, p'_μ and an emitted photon k'_μ means that, squaring both sides and using $k'^2_\mu = 0$

$$m^2 + p \cdot p' = 0\,. \tag{1.1}$$

This relation is impossible to fulfil since

$$p \cdot p' > m^2 \tag{1.2}$$

1 http://www.extreme-light-infrastructure.eu/

2 http://www.xfel.eu/

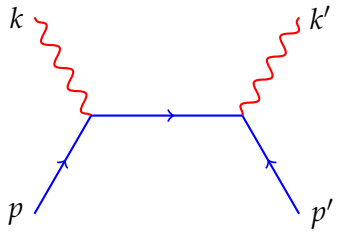

Figure 2: Pair annihilation in vacuum, with two emitted photons.

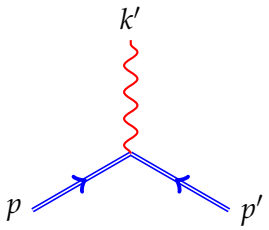

Figure 3: Feynman diagram for the one-photon channel in pair annihilation. Again double lines indicate particles in background fields.

which clearly violates (1.1). To lowest order then, pair annihilation must create at least two photons k_μ and k'_μ to conserve four-momentum. This process is visualised in Figure 2.

However, in background fields the one-photon channel opens up since the incoming particles may interact with some number n of photons k_μ in the laser, that is the process $p_\mu + p'_\mu + nk_\mu = k'_\mu$. Squaring this momentum conversation then means

$$n = -\frac{(p_\mu + p'_\mu)^2}{2k \cdot (p + p')}, \tag{1.3}$$

an equation which will be covered in more detail later on. The Feynman diagram for this process is shown in Figure 3.

1.2 SECOND ORDER PROCESSES

When coupling matter to photons in QED, each coupling brings with it a factor of $\alpha = 1/137$. Thus the two-photon coupling in Figure 2 is far more likely to occur than the process in which three photons are emitted and in general, only the first few orders need to be included in calculations.

In strong field QED this is not necessarily the case, since couplings with the background will affect the processes and laser parameters may make coupling constants larger than unity. It has been shown that for certain resonances second-order processes may be more important than first-order, but because of the difficult calculations involved they are very much outside the scope of this thesis: We only consider a single emission.

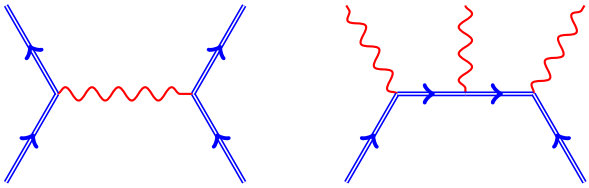

Figure 4: A few higher-order processes in background fields.

For a treatment of second-order effects, see [10].

1.3 NOTATION

Throughout the report natural units are used, setting $\hbar = c = 1$ with $\hbar$ being the reduced Planck constant and c the speed of light in vacuum. For four-vectors the metric $\eta_{\mu\nu} = \eta^{\mu\nu} = \mathrm{diag}(1, -1, -1, -1)$ is used and scalar products are written as $p \cdot x = \eta_{\mu\nu} p^\mu x^\nu$. The specific product of Dirac γ-matrices and four-vectors is denoted by the usual Feynman slash as $\gamma \cdot p = \not{p}$.

2

PARTICLES IN STRONG FIELDS

Models for particles in background fields range back to the early years of Quantum Mechanics. This chapter gives an overview of the physics involved, starting with how one includes such fields in the theory, early attempts to solve the problem by considering infinite plane wave-backgrounds and the modern struggle to shape those fields into laser pulses. We finally arrive at the cross section for one-photon emission by pair annihilation in background fields of plane waves.

2.1 VOLKOV ELECTRONS AND THE SCATTERING MATRIX

To develop the theory used in this project, we first need to understand how background fields affect particles, what form the scattering matrix takes and how to go from it to the cross section, a physical quantity that can be measured.

In ordinary Quantum Electrodynamics, the theory stems from the Lagrangian density [9]

$$\mathcal{L} = -\frac{1}{4} F_{\mu\nu} F^{\mu\nu} + \bar{\psi} \left(i \not{D} - m \right) \psi \,, \tag{2.1}$$

where the photon field A_μ is included in the field tensors $F_{\mu\nu}$ and the covariant derivative D_μ as

$$F_{\mu\nu} = \partial_\mu A_\nu - \partial_\nu A_\mu \tag{2.2}$$

$$D_\mu = \partial_\mu + ieA_\mu \,, \tag{2.3}$$

ψ, $\bar{\psi}$ are the usual Dirac spinors for fermions and m the electron mass. An external laser field $\mathcal{A}_\mu$ can be incorporated simply by translating the photon field in this action (see [11] and references therein), ending up with

$$D_\mu \to \partial_\mu + ieA_\mu + ie\mathcal{A}_\mu \,. \tag{2.4}$$

This added term modifies the electron propagator, which becomes *dressed* by the laser field, represented schematically in Feynman diagrams as the coupling expansion seen in Figure 5. Here a problem arises in that there exist fields, for example high-intensity laser fields, where individual couplings are larger than unity, meaning that it is not always possible to treat these couplings perturbatively as is usually done in QED.

However, although a general treatment of background fields is difficult, there also exist fields in which fermion propagators and

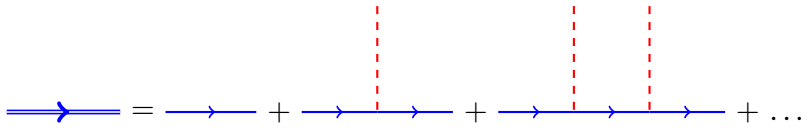

Figure 5: The electron propagator dressed by a background field, represented as a coupling expansion. Background field photons are shown as dashed lines.

external lines actually can be treated *exactly*. For background fields consisting of planar waves this is the case; Amputated external lines are given exactly by so called *Volkov wave functions*, known as [10, 12, 13]

$$\Psi_p = \left(1 + \frac{e}{2k\cdot p} \not{k} \not{\mathcal{A}}(\varphi)\right) u_p \, e^{iS(\varphi)} \tag{2.5}$$

$$S(\varphi) = -p\cdot x - \int_{-\infty}^{\varphi} \mathrm{d}\vartheta \left\{ \frac{ep\cdot\mathcal{A}(\vartheta)}{k\cdot p} - \frac{e^2\mathcal{A}(\vartheta)^2}{2k\cdot p} \right\}, \tag{2.6}$$

where k_μ and p_μ are the background photon and electron four-momenta respectively, $\mathcal{A} = \mathcal{A}(\varphi)$ again the laser field four-potential now depending on the phase $\varphi = k\cdot x$, e the electron charge and u_p the ordinary electron spinor. In this way, we can treat scattering matrix elements exactly and non-perturbatively in the field coupling. As a note, the lower integration limit in S can be changed arbitrarily from $-\infty$ as this only changes an overall phase which cancels in the squared matrix element going into actual physical quantities [14].

Using these Volkov wave functions, the scattering matrix S_{fi} can be read off and written down from the Feynman diagram of the process as shown earlier (see Figure 3) in position space as

$$\mathrm{S}_{fi} = -ie \int \mathrm{d}^4x \, \bar{\Psi}_{-p'} \not{\varepsilon} \, \Psi_p \, e^{ik'\cdot x} \tag{2.7}$$

for incoming electron-positron pair p_μ, p'_μ and emitted photon k'_μ with polarisation ε_μ. With this scattering matrix in mind, we go to a cross section for the reaction by taking the absolute square, dividing over the pulse volume V, duration T and incoming energy flux $4I$ for

$$I = \sqrt{(p\cdot p')^2 - m^4}\,, \tag{2.8}$$

averaging over spins, summing over outgoing polarisations and integrating over the outgoing momenta [12]:

$$\sigma = \frac{1}{16I}\frac{1}{VT}\sum_{\text{spins}}\sum_{\text{pol}}\int \frac{\mathrm{d}^3k'}{(2\pi)^3}\frac{1}{2k'_0}\,|\mathrm{S}_{fi}|^2 \tag{2.9}$$

This is the general formula for one-photon emission by pair annihilation.

2.2 ONE-PHOTON EMISSION IN INFINITE PLANE WAVES

Emission of photons in laser backgrounds was treated in the beginning of the 1960's, in the approximation of lasers as periodic plane wave backgrounds, or infinite laser pulse duration [15, 16, 17]. As the solution offers numerous similarities to the more realistic case of shaped pulses, and indeed motivates that case, it will be covered briefly. First, the laser is directed along the x^3 axis

$$k_\mu = m\nu(1,0,0,1) \tag{2.10}$$

where a dimensionless laser frequency

$$\nu = \frac{\omega}{m} \tag{2.11}$$

has been defined for the frequency ω of the laser photons. Then taking the simplest case of circular polarisation, the background is defined as

$$\mathcal{A}_\mu = a^1_\mu \cos(\varphi) + a^2_\mu \sin(\varphi)\,, \tag{2.12}$$

where

$$\begin{aligned} a^1_\mu &= \frac{ma_0}{e}(0,1,0,0) \\ a^2_\mu &= \frac{ma_0}{e}(0,0,1,0) \end{aligned} \tag{2.13}$$

are polarisation vectors and a_0 is a dimensionless laser amplitude given by the ratio between the energy gained by an electron across a laser photon wavelength λ in an electric field E to its rest mass [18]

$$a_0 = \frac{eE\lambda}{m}\,. \tag{2.14}$$

This gives the term S (2.6) as

$$S = -e\left(\frac{a^1\cdot p}{k\cdot p}\right)\sin(\varphi) + e\left(\frac{a^2\cdot p}{k\cdot p}\right)\cos(\varphi) - q\cdot x\,, \tag{2.15}$$

where q_μ is introduced as the *quasi-momentum* that charged particles pick up in constant fields, defined by

$$\begin{aligned} q^2 &= m^2(1+a_0^2) \\ &= m^{*2}\,. \end{aligned} \tag{2.16}$$

m^* is called the *effective mass* of the particles. The integrand in the scattering matrix (2.7) thus consists of the terms

$$e^{-i[\alpha_1\sin(\varphi)-\alpha_2\cos(\varphi)]} \tag{2.17}$$

$$\cos(\varphi)\, e^{-i[\alpha_1\sin(\varphi)-\alpha_2\cos(\varphi)]} \tag{2.18}$$

$$\sin(\varphi)\, e^{-i[\alpha_1\sin(\varphi)-\alpha_2\cos(\varphi)]} \tag{2.19}$$

with a common exponential prefactor $\exp[i(k' - q - q') \cdot x]$ and where the factors $\alpha_{1,2}$ have been introduced as

$$\alpha_{1,2} = e \left(\frac{a^{1,2} \cdot p}{k \cdot p} - \frac{a^{1,2} \cdot p'}{k \cdot p'} \right) . \tag{2.20}$$

The terms (2.17-2.19) can be expanded into Fourier series, for the first one noting that

$$\begin{aligned} e^{-i[\alpha_1 \sin(\varphi) - \alpha_2 \cos(\varphi)]} &= e^{-iz \sin(\varphi - \varphi_0)} \\ &= \sum_{-\infty}^{\infty} B_n \, e^{-in\varphi} \end{aligned} \tag{2.21}$$

where

$$z = \sqrt{\alpha_1^2 + \alpha_2^2} \tag{2.22}$$

$$\varphi_0 = \arccos\left(\frac{\alpha_1}{z}\right) \tag{2.23}$$

and the coefficients B_n are precisely defined in terms of Bessel functions J_n as

$$B_n = J_n(z) \, e^{in\varphi_0} . \tag{2.24}$$

Similarly, (2.18) and (2.19) can be written with coefficients

$$B_{1n} = \frac{1}{2} \left[J_{n+1}(z) \, e^{i(n+1)\varphi_0} + J_{n-1}(z) \, e^{i(n-1)\varphi_0} \right] \tag{2.25}$$

$$B_{2n} = \frac{1}{2i} \left[J_{n+1}(z) \, e^{i(n+1)\varphi_0} - J_{n-1}(z) \, e^{i(n-1)\varphi_0} \right] \tag{2.26}$$

respectively.

To summarise, the scattering matrix (2.7) has been rewritten as a sum over Bessel functions, with an exponential prefactor now of the form

$$e^{i[(k' - q - q' - nk) \cdot x]} \tag{2.27}$$

containing all the dependence of x in the integrand. Squaring this matrix and inserting it into the cross section formula (2.9) lets us perform the integrals and, jumping over the details, arrive at a cross section of the form

$$\sigma = \sum_n M_n \, \delta^{(4)}(nk_\mu + q_\mu + q'_\mu = k'_\mu) \tag{2.28}$$

for some unspecified elements M_n, the exponential prefactor having been turned into a delta function. This then is an infinite sum, each term describing momentum conservation[1], and

1 The momentum conservation in this case contains the quasi-momenta q_μ, q'_μ of the incoming particles as introduced in (2.16). This gives the emitted photon momenta k'_μ a dependence on the intensity a_0, or the effective mass m^*. Later on we will see that this dependence disappears when considering more realistic laser pulses.

is unphysical – we expect a physical result not to take the appearance of delta functions. These delta functions are an artifact from considering the background laser as an infinite plane wave. To arrive at a finite cross section we need to *shape our laser background into finite pulses*.

2.3 FINITE LASER PULSES

As seen in the previous section a laser background modeled by an infinite plane wave is problematic. A more realistic approach which as it turns out solves these problems is taking *pulse shapes* into account.

The presented theory for laser pulses in this section is built around intense laser fields with neglected transverse size effects, again approximated as plane waves only dependent on the phase $\varphi = k \cdot x$. We again direct the laser along the x^3 axis, with photon momenta k_μ as in (2.10). The background field is also again circularly polarised, but now given by the four-potential

$$\mathcal{A}_\mu = a_\mu^1 f_1(\varphi) + a_\mu^2 f_2(\varphi) \tag{2.29}$$

where $f_{1,2}(\varphi)$ are functions shaping our laser pulses. The laser field tensor is then given by

$$\mathcal{F}_{\mu\nu} = f_j'(\varphi)(k_\mu a_\nu^j - k_\nu a_\mu^j) \tag{2.30}$$

with the prime denoting derivation with respect to φ and equal indices $j = 1, 2$ are summed over.

Our laser pulses are shaped by setting [19]

$$f_1(\varphi) = \cos(\varphi)\sin^4\left(\frac{\varphi}{2N}\right) \tag{2.31}$$

$$f_2(\varphi) = \sin(\varphi)\sin^4\left(\frac{\varphi}{2N}\right) \tag{2.32}$$

for $\varphi \in \{0, 2\pi N\}$, 0 otherwise, with N then defining the number of oscillations of the field in a pulse. For convenience we also define

$$f_3(\varphi) = f_1(\varphi)^2 + f_2(\varphi)^2 \tag{2.33}$$

since it will appear in many calculations.

2.4 ONE-PHOTON EMISSION IN LASER PULSES

With a more realistic laser background defined, we again turn to calculating a cross section for the reaction. The new approach will solve the problems encountered for the infinite plane wave case, but introduce additional computational difficulties.

Again starting from the scattering matrix (2.7), but keeping $f_{1,2}(\varphi)$ non-trivial we can no longer easily expand the integrand

into sums over Bessel functions as before. Instead, we Fourier transform the non-trivial φ dependence that appears in the exponential (2.6), introducing the Fourier conjugate variable l

$$S_{fi} = -ie \int \mathrm{d}^4x \int \frac{\mathrm{d}l}{2\pi} e^{i(k'-lk-p-p')\cdot x} \varepsilon'^{\mu} \Gamma_\mu(l)\,, \tag{2.34}$$

the introduced term $\Gamma_\mu(l)$ containing this φ dependence. It is given by

$$\Gamma_\mu(l) = \int \mathrm{d}\varphi\, \bar{v}_{p'} \left[1 - \frac{e \not{\mathcal{A}}(\varphi) \not{k}}{2k\cdot p'}\right] \gamma_\mu \left[1 + \frac{e \not{k} \not{\mathcal{A}}(\varphi)}{2k\cdot p}\right] u_p \times e^{il\varphi - i\alpha_j \int_0^\varphi \mathrm{d}\vartheta\, f_j(\vartheta)}\,, \tag{2.35}$$

summing over $j = 1,2,3$ in the exponential. Apart from the previously seen $\alpha_{1,2}$ (2.20), an additional parameter α_3 has been introduced by noting that

$$\mathcal{A}(\varphi)^2 = -\frac{m^2 a_0^2}{e^2} f_3(\varphi)\,. \tag{2.36}$$

and hence setting

$$\alpha_3 = \frac{m^2 a_0^2}{2} \left(\frac{1}{k\cdot p} + \frac{1}{k\cdot p'}\right)\,. \tag{2.37}$$

Returning to our scattering matrix (2.34) the integral over d^4x can be performed, as before acquiring a delta function for momentum conservation

$$S_{fi} = -ie \int \frac{\mathrm{d}l}{2\pi} (2\pi)^4 \delta^{(4)}(lk_\mu + p_\mu + p'_\mu = k'_\mu)\, \varepsilon'^{\nu} \Gamma_\nu(l)\,, \tag{2.38}$$

the difference to (2.28) being that the effective mass q no longer appears since the particles are not in a constant presence of fields. Consider the physics of the momentum conservation in this scattering matrix: Squaring both sides of the conservation equation we find that

$$l = -\frac{(p_\mu + p'_\mu)^2}{2k\cdot(p+p')}\,, \tag{2.39}$$

thus l is completely determined by the laser and incoming particle momenta, all of which are fully known when performing experiments. l is always negative and not generally an integer. The laser background "absorbs" momentum $-lk_\mu$ from the incoming particles p and p', which then emit a new photon with momentum k'_μ.

Moving on, we define *lightfront coordinates* in position and momentum space as

$$x^\pm = x^0 \pm x^3 \tag{2.40}$$

$$x^\perp = x^1, x^2 \tag{2.41}$$

$$p_\pm = \frac{1}{2}(p_0 \pm p_3) \tag{2.42}$$

$$p_\perp = p_1, p_2 \tag{2.43}$$

respectively. Additionally, integration elements transform as

$$\mathrm{d}^4x = \frac{1}{2}\,\mathrm{d}x^+\mathrm{d}x^{\perp,-} \tag{2.44}$$

$$\mathrm{d}^4p = 2\,\mathrm{d}p_+\mathrm{d}p_{\perp,-} \tag{2.45}$$

and delta functions in momentum space as

$$\begin{aligned}\delta^{(4)}(p_\mu) &= \frac{1}{2}\delta(p_+)\delta^{(2)}(p_\perp)\delta(p_-)\\ &\equiv \frac{1}{2}\delta(p_+)\delta^{\perp,-}(p)\,,\end{aligned} \tag{2.46}$$

defining some shorthand notation in the last line. Then taking the laser photon momenta $k_\mu = (k_+, 0, 0, 0)$ and the absolute square of (2.38) it is possible to perform the integral over l for either S_{fi} or its complex conjugate. This leaves the squared amplitude as

$$\begin{aligned}|\mathrm{S}_{fi}|^2 = e^2 \int \frac{\mathrm{d}l}{2\pi}\frac{(2\pi)^8}{2\pi}\delta^{(4)}(lk_\mu + p_\mu + p'_\mu = k'_\mu)\frac{\delta^{\perp,-}(0)}{2k_+}\\ \times \varepsilon^\mu\varepsilon^{\nu *}\Gamma_\mu(l)\Gamma^*_\nu(l)\,.\end{aligned} \tag{2.47}$$

The divergent delta function $\delta^{\perp,-}(0)$ is removed by calculating the pulse volume and duration, which appear in the cross section (2.9):

$$\begin{aligned}VT &= \int_{\text{pulse}} \mathrm{d}^4x\\ &= \frac{1}{2}\int_{-\infty}^{\infty}\mathrm{d}^3x^{\perp,-}\int_{\text{pulse}}\mathrm{d}x^+\\ &= \frac{1}{2}\int_{-\infty}^{\infty}\mathrm{d}^3x^{\perp,-}\int_0^{2\pi N}\frac{\mathrm{d}(k\cdot x)}{k_+}\\ &= \frac{2\pi N}{2k_+}(2\pi)^3\delta^{\perp,-}(0)\end{aligned} \tag{2.48}$$

where $2\pi N$ is the Lorentz invariant duration and N again the number of oscillations of the field of the pulse in $k \cdot x$.

The cross section for our considered reaction becomes

$$\begin{aligned}\sigma = \frac{e^2}{16I}\frac{1}{2\pi N}\int\frac{\mathrm{d}l}{2\pi}\int\frac{\mathrm{d}^3k'}{(2\pi)^3}\frac{1}{2k'_0}\\ \times (2\pi)^4\delta^{(4)}(lk_\mu + p_\mu + p'_\mu = k'_\mu)\,\mathcal{J}\,,\end{aligned} \tag{2.49}$$

where $\mathcal{J}$ contains all the dependence on the pulse profile and is given by

$$\mathcal{J} = -\sum_{\text{spins}}\Gamma^*_\mu(l)\Gamma^\mu(l)\,, \tag{2.50}$$

for convenience absorbing a minus sign from the polarisation sum

$$\sum_{\text{pol}}\varepsilon^\mu\varepsilon^{\nu *} = -\eta^{\mu\nu} \tag{2.51}$$

which has been performed. The cross sections contains four integrals and four δ-functions, making the integrals trivial to perform. But first the expression for $\mathcal{J}$ must be studied.

Γ_μ can be rewritten as

$$\Gamma_\mu(l) = \bar{v}_{p'} T_\mu u_p \,, \tag{2.52}$$

where T_μ is introduced as a collection of the individual terms in the function,

$$\begin{aligned} T_\mu = \gamma_\mu B_0 + e\left(\frac{\gamma_\mu \not{k} \not{a}^1}{2k\cdot p} - \frac{\not{a}^1 \not{k} \gamma_\mu}{2k\cdot p'}\right) B_1 \\ + e\left(\frac{\gamma_\mu \not{k} \not{a}^2}{2k\cdot p} - \frac{\not{a}^2 \not{k} \gamma_\mu}{2k\cdot p'}\right) B_2 - \left(\frac{m^2 a_0^2 k_\mu \not{k}}{2(k\cdot p)(k\cdot p')}\right) B_3 \,. \end{aligned} \tag{2.53}$$

Here, the functions B_j have been introduced as

$$B_j = \int \mathrm{d}\varphi\, f_j(\varphi)\, e^{il\varphi - i\alpha_k \int_0^\varphi \mathrm{d}\vartheta\, f_k(\vartheta)} \tag{2.54}$$

for $j,k = 1,2,3$. The last term B_0 is defined as

$$B_0 = \int \mathrm{d}\varphi\, e^{il\varphi - i\alpha_k \int_0^\varphi \mathrm{d}\vartheta\, f_k(\vartheta)} \tag{2.55}$$

which in contrast to (2.54) seems to diverge since there is no shaping envelope in the integrand. However, regulating the expression in a gauge invariant manner gives [6]

$$B_0 = \frac{\alpha_j B_j}{l} \tag{2.56}$$

with a sum as usual going over $j = 1,2,3$, giving a convergent expression for this and thus all terms B.

With all these quantities in place, the sum over spins in (2.50) can be performed and a trace is obtained:

$$\begin{aligned} \mathcal{J} &= -\sum_{\text{spins}} \bar{u}_p T_\mu^* v_{p'} \bar{v}_{p'} T^\mu u_p \\ &= -\operatorname{tr}\left[(\not{p} + m) T_\mu^* (\not{p}' - m) T^\mu\right] \end{aligned} \tag{2.57}$$

This trace can be performed[2], resulting in 24 non-zero terms

$$\begin{aligned} \mathcal{J} = (16m^2 + 8p\cdot p')|B_0|^2 \\ - 4m^2 a_0^2 \left(\frac{k\cdot p}{k\cdot p'} + \frac{k\cdot p'}{k\cdot p}\right)\left(|B_1|^2 + |B_2|^2\right) \\ + 4e\left(\frac{k\cdot p'}{k\cdot p} p - \frac{k\cdot p}{k\cdot p'} p' + p - p'\right)\cdot a^1 \left(B_1 B_0^* + \text{c. c.}\right) \\ + 4e\left(\frac{k\cdot p'}{k\cdot p} p - \frac{k\cdot p}{k\cdot p'} p' + p - p'\right)\cdot a^2 \left(B_2 B_0^* + \text{c. c.}\right) \\ + 4m^2 a_0^2 (B_0^* B_3 + \text{c. c.}) \,, \end{aligned} \tag{2.58}$$

2 For instance using FORM, a powerful program well suited for calculating traces. Available at `http://www.nikhef.nl/~form/`.

easily rewritten to

$$\begin{aligned}\mathcal{J} = &(16m^2 + 8p\cdot p')|B_0|^2 \\ &+ 8m^2a_0^2(2u-1)\left(|B_1|^2 + |B_2|^2\right) \\ &+ 4k\cdot k'\left[(\alpha_1 B_1 + \alpha_2 B_2)B_0^* + \text{c. c.}\right] \\ &+ 4m^2a_0^2\left(B_0^* B_3 + \text{c. c.}\right)\end{aligned} \tag{2.59}$$

by using α_j as introduced earlier and simplifying the expression by introducing

$$\begin{aligned}u &= \frac{(k\cdot k')^2}{4(k\cdot p)(k\cdot p')} \\ &= \frac{[k\cdot(p+p')]^2}{4(k\cdot p)(k\cdot p')}\,,\end{aligned} \tag{2.60}$$

in the last line having used that the delta function in (2.49) will set $k'_\mu = lk_\mu + p_\mu + p'_\mu$. The definition of B_0 (2.56) gives that

$$\alpha_1 B_1 + \alpha_2 B_2 = lB_0 - \alpha_3 B_3 \tag{2.61}$$

which after some easy algebra in turn gives

$$\begin{aligned}\mathcal{J} = &8m^2|B_0|^2 \\ &+ 4m^2a_0^2(2u-1)\left[2|B_1|^2 + 2|B_2|^2 - (B_0^* B_3 + \text{c. c.})\right]\,,\end{aligned} \tag{2.62}$$

which is the final expression for the term.

2.5 CROSS SECTION FOR ONE-PHOTON EMISSION

Inserting $\mathcal{J}$ (2.62) into the formula for the cross section (2.49) and trivially performing the integrals by using the delta function we finally arrive at an *exact* formula:

$$\sigma = \frac{1}{4I}\frac{e^2m^2}{2k\cdot k'}\frac{1}{2\pi N}Z\,, \tag{2.63}$$

with I given by (2.8) and

$$Z = 2|B_0|^2 + a_0^2(2u-1)\left[2|B_1|^2 + 2|B_2|^2 - (B_0^* B_3 + \text{c. c.})\right]\,. \tag{2.64}$$

Functions B_j are given by (2.54) and B_0 by (2.56). The integrals in these functions will converge due to the finite supports of $f_j(\varphi)$ and we have escaped the infinite sum of the cross section with an infinite plane wave background (2.28).

Solving the integrals B_j is still a difficult task, but in the following chapters we use approximations well suited for modern lasers to estimate them.

3 THE XFEL REGIME

Considering the in-development European XFEL facility, we deal with ultrashort, highly energetic X-ray laser pulses. Currently, the facility is planned to begin operating in 2014 and experimenting in 2015.

Pulse duration (fs)	ω (keV)	a_0
< 100	$0.2 - 12$	$0.1 - 10$

Table 1: Laser parameters at the XFEL facility.

3.1 XFEL LASER PARAMETERS

For the purposes of these calculations, the parameters used to model the XFEL laser have been set as

$$\nu = 10^{-2} \tag{3.1}$$
$$N = 1.2 \times 10^5 \,, \tag{3.2}$$

corresponding to pulses of 100 fs duration with frequency $\omega = 5\,\text{keV}$. a_0 takes values starting from 0.1 to the goal intensity 10 [20] and the pulse envelopes are defined as in Section 2.3. The pulse is visualised in Figure 6.

The kinematics of the incoming electron-positron pair (introduced and studied for an optical laser in [21]) is detailed in Figure 7 and consists of the pair coming in anti-parallel to the laser with only a very small offset angle θ. We later also consider the limiting case of the pair coming in transverse to the laser, i. e. for $\theta = 90^\circ$.

We then have incoming laser photons and particle pair

$$k_\mu = m\nu(1, 0, 0, 1) \tag{3.3}$$
$$p_\mu = m\gamma(1, \beta\sin\theta\cos\phi, \beta\sin\theta\sin\phi, -\beta\cos\theta) \tag{3.4}$$
$$p'_\mu = m\gamma(1, -\beta\sin\theta\cos\phi, -\beta\sin\theta\sin\phi, -\beta\cos\theta)\,, \tag{3.5}$$

with a particle energy scale set by the linear accelerator in the XFEL facility at DESY

$$\gamma = 80 \tag{3.6}$$

and $\beta = \sqrt{1 - 1/\gamma^2}$. ϕ is the azimuthal angle that the particle pair makes to the laser polarisation basis. Momentum conservation in (2.38) then gives (2.39) as

$$l = -\frac{\gamma}{\nu}(1 - \beta\cos\theta) \tag{3.7}$$

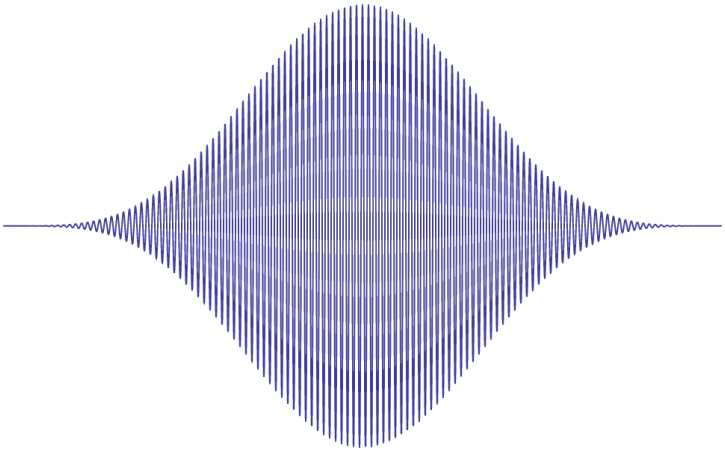

Figure 6: A typical laser pulse at the XFEL facility. Due to the high photon frequency the femtosecond short pulses still contain a large number of periods.

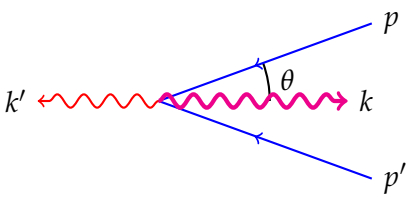

Figure 7: Kinematics of the considered process for one-photon pair annihilation in the lab frame.

and

$$k'_\mu = m\gamma(1+\beta\cos\theta)(1,0,0,-1)\,. \tag{3.8}$$

The emitted photons are backscattered against the laser. Other required parameters are

$$\alpha_1 = -\frac{2a_0\beta}{\nu}\frac{\sin\theta\cos\phi}{1+\beta\cos\theta} \tag{3.9}$$

$$\alpha_2 = -\frac{2a_0\beta}{\nu}\frac{\sin\theta\sin\phi}{1+\beta\cos\theta} \tag{3.10}$$

$$\alpha_3 = \frac{a_0^2}{\nu\gamma}\frac{1}{1+\beta\cos\theta} \tag{3.11}$$

and

$$u = 1\,. \tag{3.12}$$

3.2 SEPARATION OF OSCILLATING INTEGRANDS

With all preliminaries in place it is time to turn to the integrals (2.54)

$$B_j = \int_0^{2\pi N} \mathrm{d}\varphi\, f_j(\varphi)\, e^{il\varphi - i\alpha_k \int_0^\varphi \mathrm{d}\vartheta\, f_k(\vartheta)} \tag{2.54}$$

which are still very difficult to solve using standard numerical integration methods because of rapid oscillations set by a huge N. There are also no stationary points in the exponent, prohibiting an easy solution using e. g. the method of steepest descent.

However, it is possible to exploit the large N to find a good approximation, since the functions $f_{1,2}$ (2.31-2.32) may be written as one rapidly oscillating part and one envelope part, giving

$$f_1(\varphi) = g(\varphi)\cos(\varphi) \tag{3.13}$$

$$f_2(\varphi) = g(\varphi)\sin(\varphi) \tag{3.14}$$

$$f_3(\varphi) = g(\varphi)^2 \tag{3.15}$$

for

$$g(\varphi) = \sin^4\left(\frac{\varphi}{2N}\right)\,. \tag{3.16}$$

The integrals in the exponential

$$F_j(\varphi) = \int_0^\varphi \mathrm{d}\vartheta\, f_j(\vartheta) \tag{3.17}$$

can then, integrating by parts and using the fact that $g'(\varphi) \sim 0$ on the integration interval, be rewritten to

$$\begin{aligned} F_1(\varphi) &= g(\varphi)\sin(\varphi) - \int_0^\varphi \mathrm{d}\vartheta\, g'(\vartheta)\sin(\vartheta) \\ &\approx g(\varphi)\sin(\varphi) \end{aligned} \tag{3.18}$$

$$F_2(\varphi) \approx -g(\varphi)\cos(\varphi) \tag{3.19}$$

Thus the integrals B_j can be written

$$B_1 \approx \int_0^{2\pi N} \mathrm{d}\varphi\, g(\varphi)\, e^{il\varphi - i\alpha_3 F_3(\varphi)} \times \cos(\varphi)\, e^{-i[\alpha_1 g(\varphi)\sin(\varphi) - \alpha_2 g(\varphi)\cos(\varphi)]} \tag{3.20}$$

$$B_2 \approx \int_0^{2\pi N} \mathrm{d}\varphi\, g(\varphi)\, e^{il\varphi - i\alpha_3 F_3(\varphi)} \times \sin(\varphi)\, e^{-i[\alpha_1 g(\varphi)\sin(\varphi) - \alpha_2 g(\varphi)\cos(\varphi)]} \tag{3.21}$$

$$B_3 \approx \int_0^{2\pi N} \mathrm{d}\varphi\, g(\varphi)^2\, e^{il\varphi - i\alpha_3 F_3(\varphi)} \times e^{-i[\alpha_1 g(\varphi)\sin(\varphi) - \alpha_2 g(\varphi)\cos(\varphi)]} \tag{3.22}$$

In these factors we recognise (2.17-2.19) from Section 2.2. Using the same trick as in that section, these integrals can be rewritten as sums over Bessel functions J_n

$$B_1 \approx \sum_n \int_0^{2\pi N} \mathrm{d}\varphi\, g(\varphi)\, e^{il\varphi - in\varphi - i\alpha_3 F_3(\varphi)} \times \frac{1}{2}\left[J_{n+1}(z)\, e^{i(n+1)\varphi_0} + J_{n-1}(z)\, e^{i(n-1)\varphi_0}\right] \tag{3.23}$$

$$B_2 \approx \sum_n \int_0^{2\pi N} \mathrm{d}\varphi\, g(\varphi)\, e^{il\varphi - in\varphi - i\alpha_3 F_3(\varphi)} \times \frac{1}{2i}\left[J_{n+1}(z)\, e^{i(n+1)\varphi_0} - J_{n-1}(z)\, e^{i(n-1)\varphi_0}\right] \tag{3.24}$$

$$B_3 \approx \sum_n \int_0^{2\pi N} \mathrm{d}\varphi\, g(\varphi)^2\, e^{il\varphi - in\varphi - i\alpha_3 F_3(\varphi)}\, J_n(z)\, e^{in\varphi_0} \tag{3.25}$$

where now (2.22-2.23) are

$$z = \frac{2a_0\beta}{\nu}\frac{\sin\theta}{1+\beta\cos\theta} g(\varphi) \tag{3.26}$$

$$\varphi_0 = \pi - \phi\,. \tag{3.27}$$

As we show in the next section, converting the integrals in this way makes them possible to solve.

3.3 SOLUTION USING THE METHOD OF STEEPEST DESCENT

Having approximated and rewritten the integrands in B_j as sums over Bessel functions (3.23-3.25), the exponential factors now contain *stationary points* when

$$\frac{\mathrm{d}}{\mathrm{d}\varphi}\left[l\varphi - n\varphi - \alpha_3 F_3(\varphi)\right] = 0 \tag{3.28}$$

is fulfilled for some n and φ. With the main contributions in integrals over rapidly oscillating functions coming from stationary points this is a condition for which the method of steepest descent (see e. g. [22]) can be applied to approximate them. For all

n that satisfies this condition for some φ the method is applied and a sum over these terms is then performed to calculate the values of the B_j's: Terms for which n does not fulfil the condition for any φ should be negligible. Finally, the total cross section is calculated using (2.63).[1]

For the laser considered here, with l as in (3.7), α_3 in (3.11) and

$$\frac{\mathrm{d}F_3}{\mathrm{d}\varphi} = g(\varphi)^2 \tag{3.29}$$

with $g(\varphi)$ in (3.16), the condition for contributing terms becomes

$$\sin^8\left(\frac{\varphi}{2N}\right) = -\frac{\nu\gamma(1+\beta\cos\theta)}{a_0^2}n - \frac{\gamma^2(1-\beta^2\cos^2\theta)}{a_0^2}\,. \tag{3.30}$$

The left hand side of this equation takes values between 0 and 1 only, giving a range within which the right hand side must lie. For specified parameters a_0, γ, etc. and it is then easy to isolate domains of θ satisfying the condition for discrete values of n. With desired domains of the angle known the integrals can thus be estimated using the method of steepest descent and finally the cross section calculated.

First studying a low laser amplitude $a_0 = 0.1$ with the values $\gamma = 80$ and $\nu = 0.01$ as chosen in Section 3.1, intervals of θ for different n's are *very* narrow and form an almost comb-like structure as seen in Figure 8. For the first peak, corresponding to $n = -1$, the resulting cross section plotted in Figure 9 shows a fine structure and is about an order of magnitude larger than that of two-photon emission in vacuum (see Figure 2, this is chosen purely as a point of reference for the size of effects). The other peaks display similar structures, but as Bessel functions J_n suffer overall exponential suppression as the order $|n|$ increases the effects rapidly decrease in importance. Only the first few terms of n are of importance.

Note that the angle ϕ against the polarisation has been chosen as 0 here, but varying it produces only negligible changes for both size and details of results.

The domains θ for different terms of n rapidly increase together with intensity a_0. For $a_0 = 1.2$ The three first terms lie very close to each other, shown in Figure 10, in total covering a range of about $\sim 1^\circ$ with a notable cross section, seen in Figure 11. Also very visible is the decrease in size of effects with increasing order $-n$.

For the XFEL goal intensity $a_0 = 10$ individual domains of θ overlap for many different n's, but again only the first few terms give actual non-negligible contributions. In Figure 12 the first

1 The results presented here were verified using the numerical methods of [23].

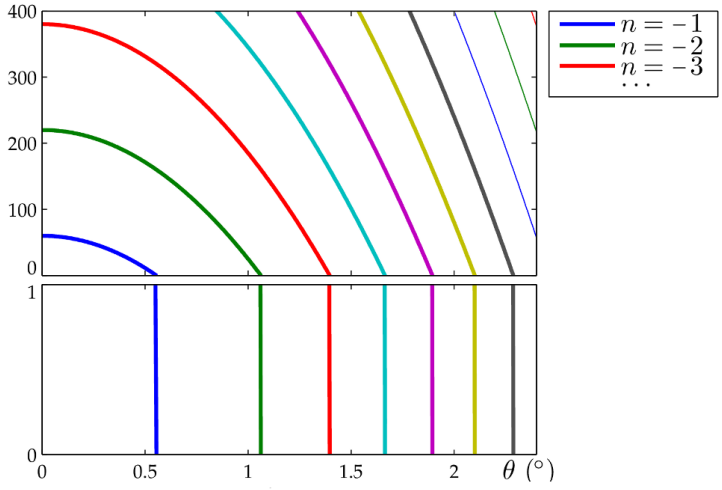

Figure 8: The right hand side of (3.30) shown as a function of θ for $a_0 = 0.1$ and a few n. The lower figure is cropped to show for which θ the functions take values between 0 and 1, fulfilling the equation for some φ. It is clear that for these parameters the cross section will only be significant in extremely narrow ranges of θ.

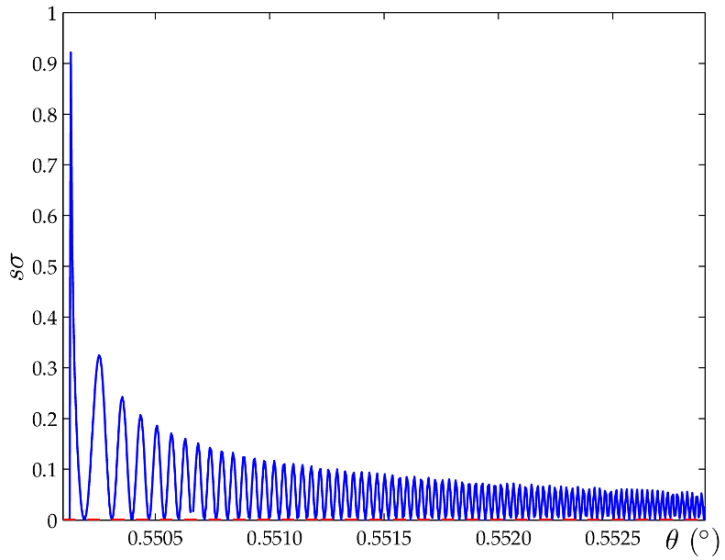

Figure 9: Studying the cross section for individual peaks in θ with $a_0 = 0.1$ reveals a fine structure, here for $n = -1$. The cross section for two-photon emission in vacuum is represented as a dashed line and barely visible. For purposes of figures the cross sections are shown multiplied by the center-of-mass energy $s = (p + p')^2$.

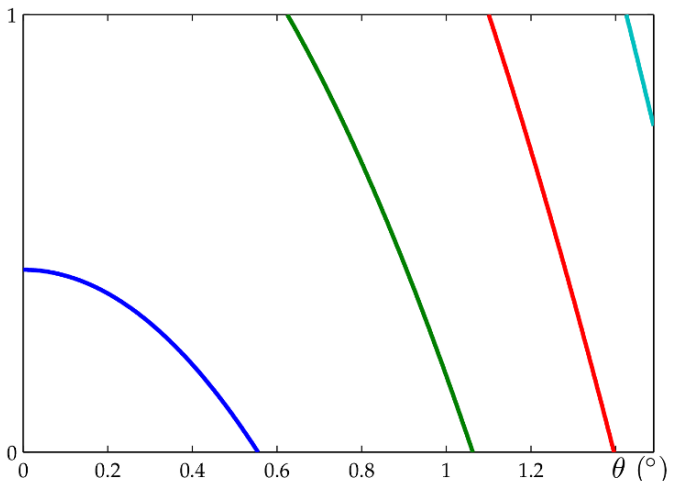

Figure 10: For $a_0 = 1.2$ the right hand side of (3.30) fulfils the equation for larger intervals of θ.

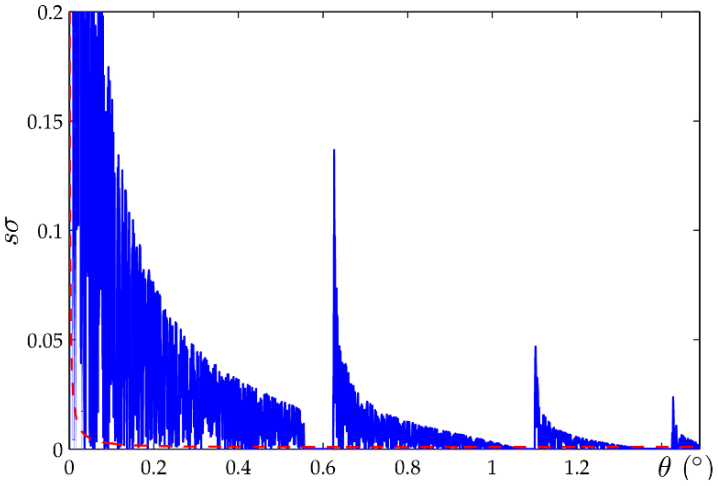

Figure 11: Again as for the lower amplitude case in Figure 9 the calculated cross section for $a_0 = 1.2$ reveals a rapidly oscillating substructure.

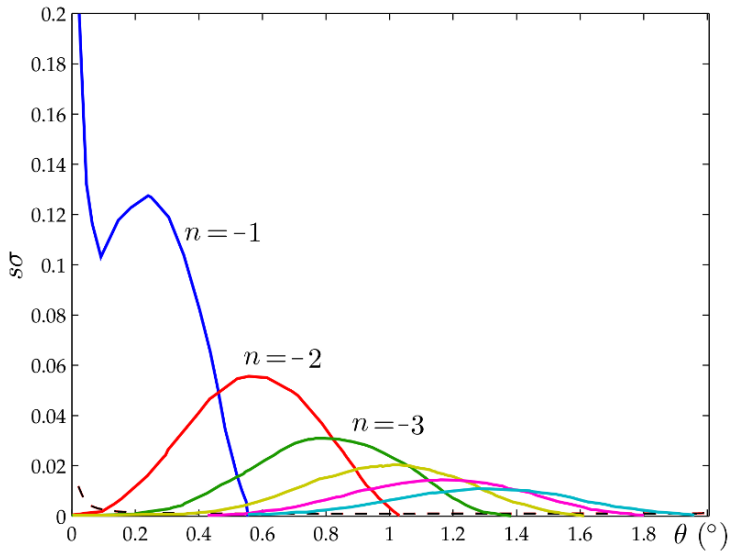

Figure 12: For $a_0 = 10$ a lot of Bessel functions contribute over ranges of θ. Here the first six, dominant terms from the sum are shown without the substructure.

and dominant contributions to the cross section are sketched to illustrate this. In total, sizable effects are now visible over a range of $\sim 2°$. While this is still requires a very finely tuned set-up and should be very difficult to detect, it has much better prospects than seen for the low intensity case considered above (Figure 9) and, as we will se in Chapter 4, also much easier than for an optical laser at ELI.

We now as promised consider the limiting case of $\theta \sim 90°$, that is the incoming particle pair hitting each other head on and perpendicular to the laser in the lab frame. For this θ the condition (3.30) gives $n \lesssim -8000$, decreasing with a_0^2. But, for n of these orders the corresponding Bessel functions give incredibly small individual contributions, meaning that the sums for the integrals B_j rapidly converge to a total cross section that should be negligible. We conclude that the cross section for this reaction, with $\theta \sim 90°$, is extremely small.

For the case of small θ up to a few degrees though, we hope that the process of single-photon emission from dressed particles will be visible if searched for in the XFEL facility.

Finally, we briefly note that precise envelope shapes in $f_{1,2}$ affect details of the cross sections as presented here but not the size. Repeating the calculation for $g(\varphi) = \sin^2(\varphi/2N)$ and $a_0 = 1.2$ gives a cross section as shown in Figure 13, to be compared to the one in Figure 11.

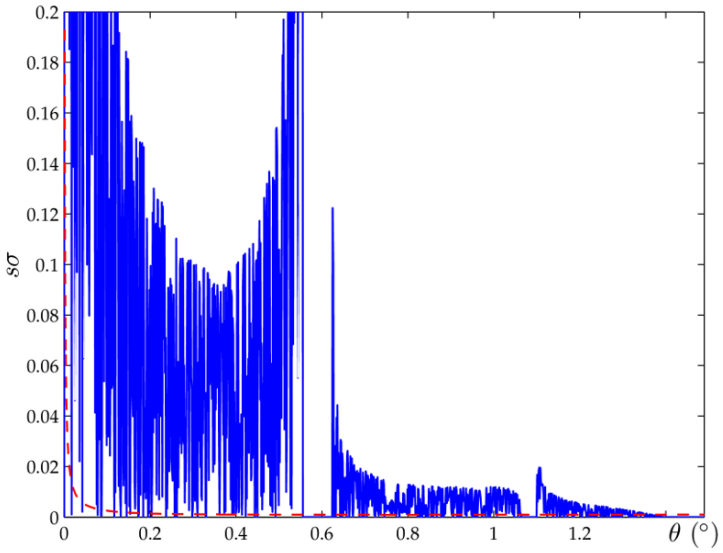

Figure 13: As expected the details of the envelope shape $g(\varphi)$ only affect details of the resulting cross section, not the size of the effect. Here shown for $a_0 = 1.2$.

4

THE OPTICAL REGIME

The optical regime that will be considered is characterised by pulses with low energies and extremely high intensities a_0. In particular, the European *Extreme Light Infrastructure* project is interesting to study since it will push laser intensities and powers to very high levels.

4.1 OPTICAL LASER PARAMETERS

Again using a laser background as described in Section 2.3, the cross section is evaluated with other parameters set as

$$a_0 = 10^4 \tag{4.1}$$

$$\nu = 2 \times 10^{-6} \tag{4.2}$$

with N assuming values between 4 and 10, corresponding to pulses of about 40 fs duration with frequency $\omega = 1\,\text{eV}$. See Figure 14. The same particle kinematics as detailed in Section 3.1 are considered, but with

$$\gamma = 10^3 \tag{4.3}$$

which is comparative to particles to be produced by linear accelerators at ELI facilities.

4.2 ESTIMATION USING INTEGRATION BY PARTS

For the laser parameters as specified here, the solution method as followed for the XFEL regime will be more difficult to motivate. For the much lower N as considered here one cannot easily approximate the envelope as basically constant over the interval. Furthermore, even for the set-up in Figure 7 that gave a notable cross section, the condition (3.30) for Bessel functions is satisfied only for large n, which suggests that the process will be difficult to detect for anything but *extremely* narrow ranges of θ as argued in the previous section (in [21] a notable cross section was found only for $\theta \sim 10^{-5}$ and with $N \gg 1$ which is not the case for these calculations).

It is possible to use another method to estimate the integrals, using integration by parts. Rewrite the integrals as

$$\begin{aligned} B_j &= \int_0^{2\pi N} \mathrm{d}\varphi\, f_j(\varphi)\, e^{ih(\varphi)} \\ &= \int_0^{2\pi N} \mathrm{d}\varphi\, f_j(\varphi) \frac{1}{ih'(\varphi)} \frac{\mathrm{d}}{\mathrm{d}\varphi}\, e^{ih(\varphi)} \end{aligned} \tag{4.4}$$

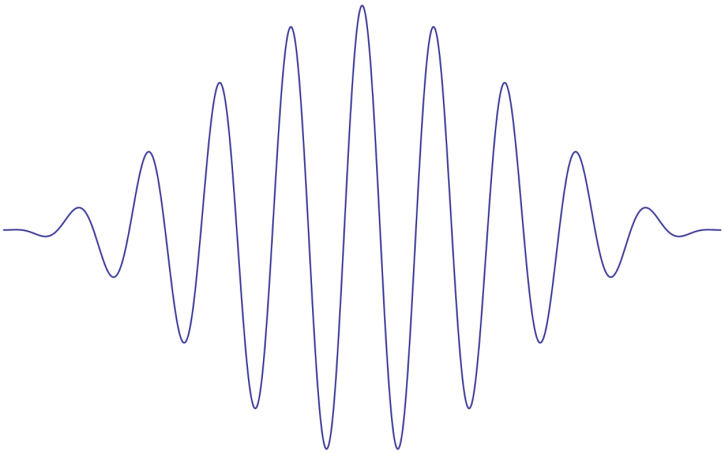

Figure 14: A typical pulse at ELI, a low frequency makes the number of periods in a pulse very low compared to XFEL lasers.

for $h'(\varphi) \neq 0$, where $h(\varphi)$ has been introduced as the oscillant

$$h(\varphi) = l\varphi - \alpha_j F_j(\varphi) \tag{4.5}$$

with F_j again being the integrated pulse shapes f_j's as in (3.17).

These integrals can be then performed as

$$\begin{aligned} B_j = & \left.\frac{f_j(\varphi)}{ih'(\varphi)}\, e^{ih(\varphi)}\right|_{\varphi=0}^{2\pi N} \\ & - \int_0^{2\pi N} \mathrm{d}\varphi\, \frac{\mathrm{d}}{\mathrm{d}\varphi}\left[\frac{f_j(\varphi)}{ih'(\varphi)}\right] e^{ih(\varphi)}\,. \end{aligned} \tag{4.6}$$

The first term is zero as the pulse envelopes $f_j(\varphi)$ are chosen to vanish smoothly at the endpoints 0 and $2\pi N$, this leaves another integral for which the procedure can be repeated like

$$\begin{aligned} B_j = 0 & - \frac{1}{ih'(\varphi)}\frac{\mathrm{d}}{\mathrm{d}\varphi}\left[\frac{f_j(\varphi)}{ih'(\varphi)}\right] e^{ih(\varphi)}\Big|_{\varphi=0}^{2\pi N} \\ & + \int_0^{2\pi N} \mathrm{d}\varphi\, \frac{\mathrm{d}}{\mathrm{d}\varphi}\left\{\frac{1}{ih'(\varphi)}\frac{\mathrm{d}}{\mathrm{d}\varphi}\left[\frac{f_j(\varphi)}{ih'(\varphi)}\right]\right\} e^{ih(\varphi)} \end{aligned} \tag{4.7}$$

and so on, every new iteration gaining nested derivatives of $f_j(\varphi)/h'(\varphi)$. The envelope $g(\varphi) = \sin^4(\varphi/2N)$ (3.16) in $f_{1,2}$ requires four iterations before creating one term that does not vanish at the end points, giving lowest-order surviving terms

$$B_{1,2} = \left.\frac{1}{[ih'(\varphi)]^5} e^{ih(\varphi)}\right|_{\varphi=0}^{2\pi N} + \mathcal{O}\left\{\frac{1}{[h'(\varphi)]^6}\right\}. \tag{4.8}$$

As f_3 contains $g(\varphi)^2$ it is also easy to see that

$$B_3 = \left.\frac{1}{[ih'(\varphi)]^9} e^{ih(\varphi)}\right|_{\varphi=0}^{2\pi N} + \mathcal{O}\left\{\frac{1}{[h'(\varphi)]^{10}}\right\}. \tag{4.9}$$

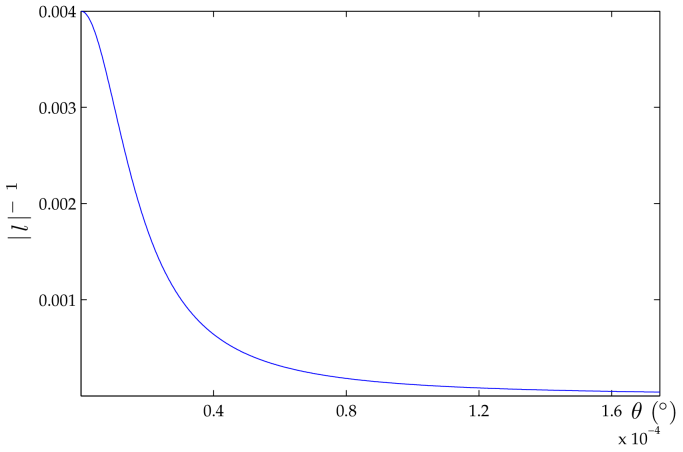

Figure 15: The angular dependence of $|l|^{-1}$, for $\gamma = 10^3$ and $\nu = 2 \times 10^{-6}$.

These terms are easily evaluated for well-defined $h(\varphi)$'s (4.5): The derivatives of F_j are just the functions f_j which again disappears at these points, thus only the first term survives the derivative and

$$\begin{aligned} h'(2\pi N) &= h'(0) \\ &= l\,. \end{aligned} \tag{4.10}$$

We thus have

$$B_{1,2} = \frac{1}{(il)^5}\left[e^{ih(2\pi N)} - 1\right] + \mathcal{O}(l^{-6}) \tag{4.11}$$

$$B_3 = \frac{1}{(il)^9}\left[e^{ih(2\pi N)} - 1\right] + \mathcal{O}(l^{-10})\,. \tag{4.12}$$

The θ dependence of these terms is kept in l and shown in Figure 15: They are maximised for $\theta = 0$, with other parameters as set earlier giving $l^{-1} \approx -1/250$ which means that the lowest order surviving terms proportional to l^{-5} are *very* small and decreasing very rapidly with θ. The case of $\theta = 90°$ gives $l^{-1} \sim 10^{-8}$.

4.3 THE OPTICAL CROSS SECTION

Even for angles θ of just fractions of degrees the cross section times the center-of-mass energy is very small. This first-order estimation gives a cross section for one-photon emission that is many orders of magnitude below the corresponding XFEL cross section for similar angles – the one-photon channel is *extremely* difficult to detect for the optical lasers at ELI.

5 CONCLUSIONS

In this report we have presented the theory of one-photon pair annihilation in background fields, a way to introduce more physical pulse shapes for lasers and a resulting formula for the cross section.

Having considered two different laser facilities with very different laser parameters, we can now present [24] that the process of one-photon emission may be a visible and verifiable effect, for a very finely tuned beam set-up. The effect has better prospects to be found in the XFEL facility, using highly energetic X-ray photons colliding with incoming, anti-parallel particles as sketched in Figure 7, than in ELI facility for optical lasers with high intensity. The cross section for XFEL parameters is shown in Figure 16.

Further developments of this theory could be to consider a non-planar wave background and its effect on the electron propagator, or various plasma effects such as an effective photon mass [25].

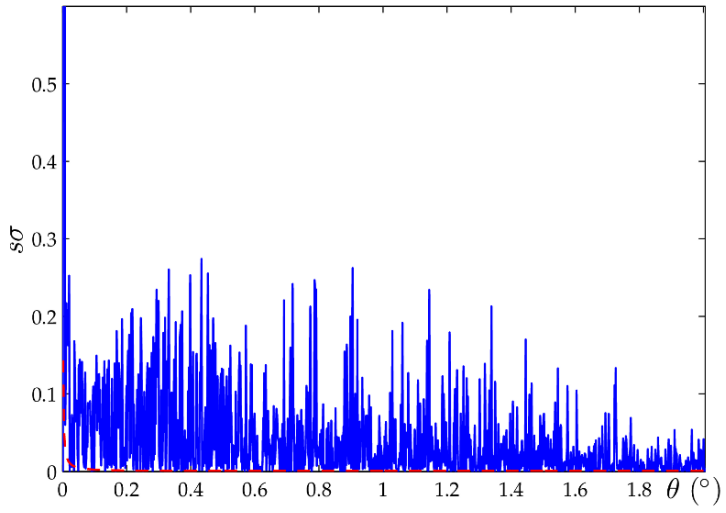

Figure 16: The total cross section for an XFEL laser with $\omega = 5\,\mathrm{keV}$, pulse duration 100 fs, intensity $a_0 = 10$ and a sum over 20 contributing Bessel functions performed as detailed in Chapter 3. Again the cross section for two-photon emission in vacuum, the dashed line, is included as a reference.

BIBLIOGRAPHY

[1] G. V. Dunne, "New strong-field QED effects at extreme light infrastructure: Nonperturbative vacuum pair production," *European Physical Journal D*, vol. 55, no. 2, pp. 327–340, 2009.

[2] J. Schwinger, "On gauge invariance and vacuum polarization," *Physical Review*, vol. 82, p. 664, 1951.

[3] T. Heinzl and A. Ilderton, "Exploring high-intensity QED at ELI," *European Physical Journal D*, vol. 55, no. 2, pp. 359–364, 2008.

[4] A. Ilderton, T. Heinzl, and M. Marklund, "Finite size effects in stimulated laser pair production," *Physics Letters B*, vol. 692, pp. 250–256, 2010.

[5] C. Bamber *et al.*, "Studies of nonlinear QED in collisions of 46.6 GeV electrons with intense laser pulses," *Physical Review D*, vol. 60, p. 092004, 1999.

[6] A. Ilderton, "Trident pair production in strong laser pulses," *Physical Review Letters*, vol. 106, no. 2, p. 020404, 2011.

[7] F. Mackenroth and A. Di Piazza, "Nonlinear Compton scattering in ultrashort laser pulses," *Physical Review A*, vol. 83, no. 3, p. 032106, 2011.

[8] S.-y. Chen, A. Maksimchuk, and D. Umstadter, "Experimental observation of relativistic nonlinear Thomson scattering," *Nature*, vol. 396, pp. 653–655, 1998.

[9] M. E. Peskin and D. V. Schroeder, *An Introduction to Quantum Field Theory*. Westview Press, 1995.

[10] A. F. Hartin, *Second Order QED Processes in an Intense Electromagnetic Field*. PhD thesis, University of London, 2006.

[11] C. Harvey, T. Heinzl, and A. Ilderton, "Signatures of high-intensity Compton scattering," *Physical Review A*, vol. 79, no. 6, p. 063407, 2009.

[12] V. B. Berestetskii, E. M. Lifshitz, and L. P. Pitaevskii, *Quantum Electrodynamics*. Pergamon Press Inc., second ed., 1982.

[13] D. M. Volkov, "Über eine Klasse von Lösungen der Diracschen Gleichung," *Zeitschrift für Physik*, vol. 94, pp. 250–260, 1935.

[14] L. S. Brown and T. W. B. Kibble, "Interaction of intense laser beams with electrons," *Physical Review*, vol. 133, no. 3, pp. 705–719, 1963.

[15] N. B. Narozhny, A. I. Nikishov, and V. I. Ritus, "Quantum processes in the field of a circularly polarized electromagnetic wave," *Zh. Eksp. Teor. Fiz.*, vol. 47, pp. 930–940, 1964. Soviet Physics JETP, 20, 622 (1965).

[16] A. I. Nikishov and V. I. Ritus, "Quantum processes in the field of a plane electromagnetic wave and in a constant field, I," *Zh. Eksp. Teor. Fiz.*, vol. 46, p. 776, 1964. Soviet Physics JETP, 19, 529 (1964).

[17] A. I. Nikishov and V. I. Ritus, "Quantum processes in the field of a plane electromagnetic wave and in a constant field, II," *Zh. Eksp. Teor. Fiz.*, vol. 46, p. 1768, 1964. Soviet Physics JETP, 19, 1191 (1964).

[18] T. Heinzl and A. Ilderton, "A Lorentz and gauge invariant measure of laser intensity," *Optics Communications*, vol. 282, no. 9, pp. 1879–1883, 2009.

[19] F. Mackenroth, A. Di Piazza, and C. H. Keitel, "Determining the carrier-envelope phase of intense few-cycle laser pulses," *Physical Review Letters*, vol. 105, no. 6, p. 063903, 2010.

[20] A. Ringwald, "Boiling the vacuum with an X-ray free electron laser." arXiv:0304.139v1, 2003.

[21] A. I. Voroshilo, E. A. Padusenko, and S. P. Roshchupkin, "One-photon annihilation of an electron-positron pair in the field of pulsed circularly polarized light wave," *Laser Physics*, vol. 20, no. 7, pp. 1679–1685, 2010.

[22] G. B. Arfken and H. J. Weber, *Mathematical Methods for Physicists*. Academic Press, fifth ed., 2001.

[23] A. J. Moylan *et al.*, "Numerical wave optics and the lensing of gravitational waves by globular clusters." arXiv:0710.3140, 2007.

[24] A. Ilderton, P. Johansson, and M. Marklund, "Pair annihilation in laser pulses: Optical vs. X-FEL regimes." arXiv:1105.3475, 2011.

[25] S. V. Bulanov *et al.*, "Interaction of electromagnetic waves with plasma in the radiation-dominated regime," *Plasma Physics Reports*, vol. 30, no. 3, pp. 196–213, 2004.